Heteroleptic Cu(I) Bis-diimine Complexes of 6,6′-Dimesityl-2,2′-bipyridine: A Structural, Theoretical and Spectroscopic Study

Michael G. Fraser, Holly van der Salm, Scott A. Cameron, Allan G. Blackman, and Keith C. Gordon*

MacDiarmid Institute for Advanced Materials and Nanotechnology, Department of Chemistry, University of Otago, Dunedin, New Zealand

Ⓢ *Supporting Information*

ABSTRACT: A series of heteroleptic Cu(I) complexes containing 6,6′-dimesityl-2,2′-bipyridine and phenanthroline-, bipyridine-, and biquinoline-based ligands is studied. The HETPHEN strategy is utilized to synthesize the heteroleptic complexes, which are stable in solution. The X-ray crystal structures of the complexes are presented; the solid-state four-coordinate Cu(I) geometries are quantified by using the τ_4 parameter. A feature of the crystal structures is the intramolecular π-stacking between the mesityl ring(s) and the diimine ligand; the phen-based complexes exhibit stacking between the phen ligand and one of the mesityl rings, creating a "Pac-Man" motif. On the other hand, the bpy-based complexes show different types of packing interaction, with both mesityl rings "clamping down" on the bpy based ligand to

give π-stacking. Cyclic voltammetry is used to examine the redox chemistry of the complexes. The most positive potentials for the oxidation process are observed for the complexes with bulky substituents ortho to the coordination nitrogens atoms, i.e., 2,9-dimethyl-1,10-phenanthroline and 6,6′-dibromo-2,2′-bipyridine. The Cu(I) MLCT transitions of the complexes are investigated by resonance Raman spectroscopy in concert with TD-DFT calculations. The resonance Raman spectra of complexes containing substituted biquinolines are straightforward, in that vibrational bands of the biquinoline-based ligand are selectively enhanced over $bpy(Mes)_2$ bands. This is consistent with the purple color of the complexes, due to the lower energy of the biquinoline-based LUMO compared to the $bpy(Mes)_2$ LUMO. All the phen- and bpy-based complexes show enhancement of $bpy(Mes)_2$ bands.
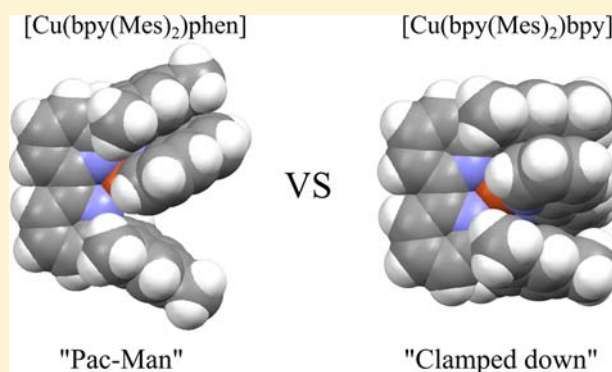
■ INTRODUCTION

Cu(I) complexes containing polypyridyl-based ligands are interesting because of their photophysical properties and their use in supramolecular assemblies.[1] Certain Cu(I) polypyridyl complexes have excited-state characteristics similar to those of ruthenium complexes such as [Ru(2,2′-bipyridine)$_3$]$^{2+}$, in that both have a long-lived charge-separated triplet excited state, originating from an MLCT transition in the visible region of the spectrum.[2] These properties make Cu(I) polypyridyl complexes potentially useful in applications such as dye-sensitized solar cells (DSSCs).[3−7] Ru(II) complexes containing carboxylic acid-substituted polypyridyl ligands are currently the most efficient TiO$_2$ sensitizers in DSSCs.[8,9] However, Cu(I) polypyridyl complexes have recently been used as sensitizers in DSSCs.[6,10−12]

One of the main drawbacks of Cu(I) complexes is their well-known lability.[13] Ligand exchange occurs rapidly in solution, often preventing the isolation of stable heteroleptic [Cu(I)-(diimine A) (diimine B)]$^+$ complexes [where diimine A and diimine B are two different ligands]. This, however, was overcome by Schmittel and colleagues by using the so-called "HETPHEN" design strategy (Figure 1).[14,15] This concept requires bulky substituents at the 2- and 9-positions of

phenanthroline, generally phenyl rings containing methyl or methoxy groups at the 2- and 6-positions. It was found that the steric bulk of the phenyl substituents prevent the formation of the bis-homoleptic Cu(I) complex.

Subsequent addition of a second, less sterically bulky phenanthroline ligand results in the desired heteroleptic complexes. Schmittel and co-workers expanded this chemistry to include heteroleptic phenanthroline complexes of the analogous d^{10} metals, Ag(I) and Zn(II).[16] It was also shown that larger groups such as anthracene and naphthalene moieties at the 2- and 9-positions also allow the formation of heteroleptic Cu(I) species.[17] This method of using sterically bulky phenanthroline ligands has been extensively exploited in the realm of supramolecular coordination chemistry.[18−24] The HETPHEN strategy can also potentially be applied to the synthesis of heteroleptic Cu(I) complexes in which one diimine ligand is an electron acceptor and the other is an electron donor ligand, capable of sustaining photoinduced electron transfer.[25] Such complexes would possess desirable photophysical properties for potential use in devices.
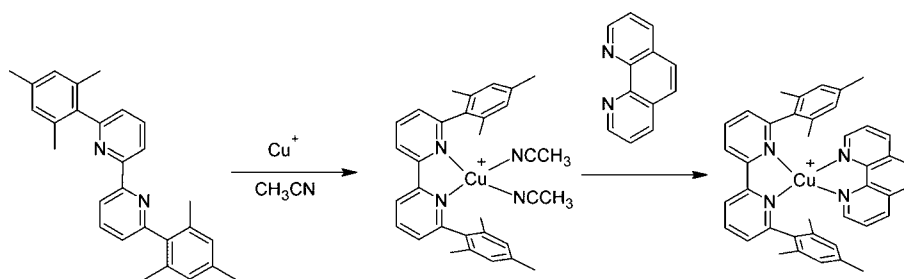
Figure 1. HETPHEN strategy using bpy(Mes)$_2$.

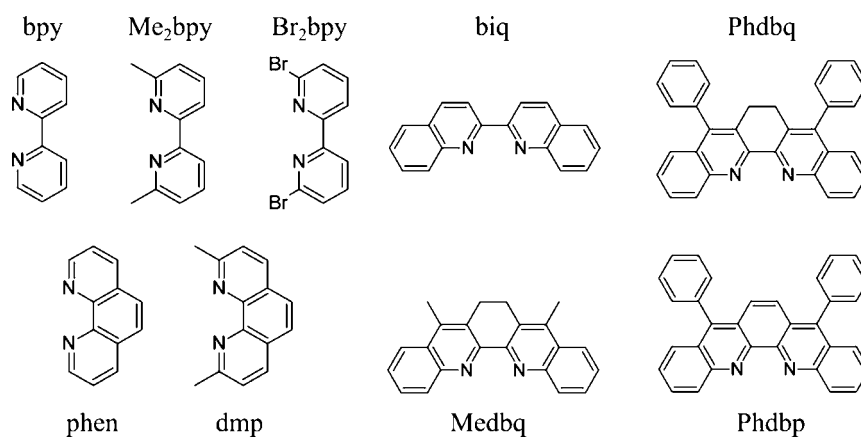**Figure 2.** Ligands used to form heteroleptic $[Cu(bpy(Mes)_2)(NN)]^+$ complexes.

A recent report by Odobel and co-workers[26] described a series of heteroleptic Cu(I) complexes based on imidazole-fused 2,9-mesityl-substituted phenanthroline ligands. The heteroleptic complexes included, among others, a 3,6-dibutyl-substituted dipyridophenazine ligand and 2,9-dimethyl-1,10-phenanthroline (dmp) as the second diimine ligand. The electronic properties of the complexes were characterized by TD-DFT calculations. All but one of the heteroleptic complexes displayed emission with nanosecond excited state lifetimes in dichloromethane solution. The complex that did not display emission was that with 1,10-phenanthroline (phen) as the second diimine ligand. The absence of sterically bulky groups at the 2- and 9-position of the phen ligand increases the likelihood of forming a exciplex between the solvent and/or counterion and the Cu(II) ion of the excited state.[27] The excited state properties resulting from MLCT excitation are determined by the electronic and structural changes on going from the ground-state Cu(I) to the excited state Cu(II). This change in oxidation state results in the flattening of the tetrahedral Cu(I) to a more "square-planar-like" geometry. In the newly formed Cu(II) species a fifth coordination site is made available, which can be bound to Lewis basic species such as counterions and solvent molecules.[2] McMillin and co-workers[27−31] studied the effect of varying solvent, counterion, and the addition of external molecules on the emission intensity and excited-state lifetime of $[Cu(dmp)_2]^+$ and other emissive $[Cu(NN)_2]^+$ complexes. These investigations showed that any factor limiting the formation of an exciplex increases the excited state lifetime of the complex. Many groups have employed ultrafast spectroscopic techniques to understand the structural changes on going from the ground to the excited state of Cu(I) polypyridyl complexes, namely, time-resolved absorption and emission spectroscopy.[32−35] The generally accepted mechanism was proposed by Tahara and co-workers[36,37] using femto-

second time-resolved emission spectroscopy. The experiments showed that the dominant excited state pathway involves the structural change (flattening distortion) occurring in the lowest energy singlet state (S_1), before intersystem crossing to the lowest energy triplet state (T_1).

This paper presents heteroleptic Cu(I) complexes of the bipyridine-based ligand 6,6′-dimesityl-2,2′-bipyridine (bpy-(Mes)$_2$) with a series of diimine-based ligands as the second nonmesityl-based ligand. This paper builds on our recent report on heteroleptic Cu(I) complexes of sulfur-substituted dipyr-idophenazine-based ligands.[38] The bpy(Mes)$_2$ ligand was first synthesized by Schmittel et al.[39] and meets the requirements for the formation of heteroleptic complexes in the same way as the more rigid 2,9-dimesitylphenanthroline ligands. The ligands chosen to coordinate to the $[Cu(bpy(Mes)_2)]^+$ unit are shown in Figure 2. These can be classified into three groups: bipyridine-based ligands [2,2-bipyridine (bpy), 6,6′-dimethyl-2,2′-bipyridine (Me$_2$bpy), and 6,6′-dibromo-2,2′-bipyridine (Br$_2$bpy)], phenanthroline-based ligands [1,10-phenanthroline (phen) and 2,9-dimethyl-1,10-phenanthroline (dmp)], and biquinoline-based ligands [2,2′-biquinoline (biq), 4,4′-diphen-yl-3,3′-dimethylene-2,2′-biquinoline (Phdbq), 4,4′-dimethyl-3,3′-dimethylene-2,2′-biquinoline (Medbq), and 5,8-diphenyl-dibenzo-1,10-phenanthroline (Phdbp)].

The ligands offer a range of structural and electronic features. In this paper, we investigate the properties of these heteroleptic Cu(I) complexes using a variety of techniques. The solid-state structures of the compounds are investigated using X-ray crystallography. The electrochemistry of the complexes are investigated, and their electronic transitions are investigated via TD-DFT calculations and resonance Raman spectroscopy.

■ EXPERIMENTAL SECTION

General. The ligands 1,10-phenanthroline, 6,6′-dimethyl-2,2′-bipyridine, 6,6′-dibromo-2,2′-bipyridine, biquinoline, 2,9-dimethyl-1,10-phenanthroline, and 2,2′-bipyridine were purchased from Aldrich and used as received. $[Cu(MeCN)_4]BF_4$ and bpy(Mes)$_2$ were synthesized according to literature methods.[39,40] The ligands Phdbq, Medbq, and Phdbp were available from previous studies.[41] The syntheses of Cu(I) complexes were carried out in a mixture of dry dichloromethane and acetonitrile, and crude products were purified by either recrystallization from methanol or ether diffusion into a concentrated dichloromethane solution of the complex. All syntheses were carried out in a similar fashion, and that of [Cu(bpy(Mes)$_2$)-(phen)]BF$_4$ is given in detail below as a typical example.

[Cu(bpy(Mes)$_2$)(phen)]BF$_4$. A 40 mg portion of bpy(Mes)$_2$ (1.02×10^{-4} mol) was dissolved in 20 mL of degassed CH$_2$Cl$_2$. To this solution, [Cu(CH$_3$CN)$_4$]BF$_4$ (32 mg, 1.02×10^{-4} mol) dissolved in a minimum volume of CH$_3$CN was then added at room temperature to give a yellow solution. This was stirred for 5 min and then 1,10-phenanthroline (18 mg, 1.02×10^{-4} mol) in a minimum volume of CH$_2$Cl$_2$ was added, and the solution immediately turned dark red. This was stirred at room temperature for 30 min, and the solvent was then removed under reduced pressure to give a red oil. This was dissolved in a minimum volume of CH$_2$Cl$_2$, and vapor diffusion of diethyl ether into the solution over 24 h affords dark red crystals suitable for X-ray crystallography: 68 mg, yield = 92%; ^{1}H NMR (400 MHz, CDCl$_3$) δ 8.57 (2H, dd, J = 8.0, 0.8 Hz), 8.48 (2H, dd, J = 4.8, 1.6 Hz), 8.42 (2H, dd, J = 8.0, 1.6 Hz), 8.25 (2H, t, J = 7.6 Hz), 7.86 (2H, s), 7.76 (2H, dd, J = 8.0, 4.8 Hz), 7.47 (2H, dd, J = 7.6, 0.8 Hz), 5.77 (4H, s), 1.68 (12H, s), 1.41 (6H, s); MS m/z (ESI POS) 635.22 {Cu(bpy(Mes)$_2$)-(phen)}$^+$. Anal. Calcd for C$_{40}$H$_{36}$N$_4$CuBF$_4$: C, 66.44; H, 5.02; N, 7.75. Found: C, 66.09; H, 5.10; N, 7.83.

[Cu(bpy(Mes)$_2$)(dmp)]BF$_4$. Recrystallized from methanol: 70 mg, yield = 92%; ^{1}H NMR (400 MHz, CDCl$_3$) δ 8.69 (2H, d, J = 8 Hz), 8.29 (2H, t, J = 8 Hz), 8.23 (2H, d, J = 8.4 Hz), 7.79 (2H, s), 7.51 (2H, d, J = 8.4 Hz), 7.45 (2H, d, J = 7.6 Hz), 5.99 (4H, s), 2.29 (6H, s), 1.66 (6H, s), 1.55 (12H, s); MS m/z (ESI POS) 663.257 {Cu(bpy(Mes)(dmp)}$^+$. Anal. Calcd for C$_{42}$H$_{40}$N$_4$CuBF$_4$: C, 67.15; H, 5.37; N, 7.46. Found: C, 66.95; H, 5.40; N, 7.43.

[Cu(bpy(Mes)$_2$)(bpy)]BF$_4$. Recrystallized from methanol: 78 mg, yield = 81%; ^{1}H NMR (400 MHz, CDCl$_3$) δ 8.50 (2H, d, J = 8 Hz), 8.22 (2H, t, J = 8 Hz), 8.08 (2H, d, J = 4.8 Hz), 7.96−7.89 (4H, m), 7.49 (2H, d, J = 8 Hz), 7.37 (2H, m), 6.10 (4H, s), 1.83 (6H, s), 1.70 (12H, s); MS m/z (ESI POS) 612.258 {(Cu(bpy(Mes)$_2$)(bpy)}$^+$. Anal. Calcd for C$_{38}$H$_{36}$N$_4$CuBF$_4$: C, 65.28; H, 5.19; N, 8.02. Found: C, 64.97; H, 5.31; N, 7.75.

[Cu(bpy(Mes)$_2$)(Me$_2$bpy)]BF$_4$. Recrystallized by ether diffusion into a dichloromethane solution of the complex: 63 mg, yield = 85%; ^{1}H NMR (400 MHz, CDCl$_3$) δ 8.61 (2H, d, J = 8.0, 0.8 Hz), 8.26 (2H, t, J = 7.6 Hz), 7.78 (4H, m), 7.49 (2H, d, J = 7.6 Hz), 7.16 (2H, t, J = 4.8 Hz), 6.28 (4H, s), 2.04 (6H, s), 1.87 (6H, s), 1.59 (12H, s); MS m/z (ESI POS) 639.25 {(Cu(bpy(Mes)(Me$_2$bpy)}$^+$. Anal. Calcd for C$_{40}$H$_{40}$N$_4$CuBF$_4$: C, 66.07; H, 5.55; N, 7.71. Found: C, 65.94; H, 5.75; N, 7.75.

[Cu(bpy(Mes)$_2$)(Br$_2$bpy)]BF$_4$. Recrystallized from methanol: 72 mg, yield = 83%; ^{1}H NMR (400 MHz, CDCl$_3$) δ 8.36 (2H, d, J = 8 Hz), 8.32 (2H, d, J = 8 Hz), 8.17 (2H, t, J = 8 Hz), 7.90 (2H, t, J = 8 Hz), 7.53 (2H, d, J = 7.6 Hz), 7.47 (2H, d, J = 8 Hz), 6.33 (4H, s), 1.89 (6H, s), 1.71 (12H, s); MS m/z (ESI POS) 769.042, {Cu(bpy-(Mes)$_2$)(Br$_2$bpy)}$^+$. Anal. Calcd for C$_{38}$H$_{34}$N$_4$Br$_2$CuBF$_4$: C, 53.46; H, 4.00; N, 6.54. Found: C, 53.19; H, 4.34; N, 6.32.

[Cu(bpy(Mes)$_2$)(biq)]BF$_4$·0.5CH$_3$OH. Recrystallized from methanol: 88 mg, yield = 87%; ^{1}H NMR (400 MHz, CDCl$_3$) δ 8.82 (2H, d, J = 8 Hz), 8.48 (2H, d, J = 8.8 Hz), 8.32 (2H, t, J = 7.6 Hz), 8.15 (2H, d, J = 8.8 Hz), 7.94 (2H, d, J = 8 Hz), 7.65−7.54 (6H, m), 7.44 (2H, d, J = 7.6 Hz), 5.69 (4H, s), 1.68 (6H, s), 1.24 (12H, s); MS m/z (ESI POS) 711.25 {(Cu(bpy(Mes)$_2$)(biq)}$^+$. Anal. Calcd for C$_{46}$H$_{40}$N$_4$CuBF$_4$·0.5CH$_3$OH: C, 68.51; H, 5.19; N, 6.87. Found: C, 68.39; H, 5.19; N, 6.87.

[Cu(bpy(Mes)$_2$)(Medbq)]BF$_4$·CH$_3$OH. Recrystallized from methanol: 70 mg, yield = 81%; ^{1}H NMR (400 MHz, CDCl$_3$) δ 8.85 (2H, d, J = 8 Hz), 8.13 (2H, d, J = 8 Hz), 8.08 (2H, d, J = 8.4 Hz), 7.62−7.58 (4H, m), 7.49 (2H, t, J = 8.4 Hz), 7.41 (2H, d, J = 7.6 Hz), 5.71 (4H, s), 3.20 (4H, s), 2.77 (6H, s), 1.67 (6H, s), 1.26 (12H, s); MS m/z (ESI POS) 765.30 {Cu(bpy(Mes)$_2$)(Medbq)}$^+$. Anal. Calcd for C$_{50}$H$_{46}$N$_4$CuBF$_4$0.5·CH$_3$OH: C, 69.77; H, 5.57; N, 6.45. Found: C, 69.72; H, 5.41; N, 6.37.

[Cu(bpy(Mes)$_2$)(Phdbq)]BF$_4$·CH$_3$OH. Recrystallized from methanol: 69 mg, yield = 69%; ^{1}H NMR (400 MHz, CDCl$_3$) δ 8.96 (2H, d, J = 8 Hz), 8.38 (2H, t, J = 7.6 Hz), 7.70 (2H, d, J = 8.4 Hz), 7.63−7.44 (14H, m), 7.33 (4H, m), 5.86 (4H, s), 2.79 (4H, s), 1.78 (6H, s), 1.35 (12, s); MS m/z (ESI POS) 889.338 {(Cu(bpy(Mes)$_2$)(Phdbq)}$^+$. Anal. Calcd for C$_{60}$H$_{50}$N$_4$CuBF$_4$·CH$_3$OH: C, 72.68; H, 5.39; N, 5.55. Found: C, 72.86; H, 5.27; N, 5.66.

[Cu(bpy(Mes)$_2$)(Phdbp)]BF$_4$. Recrystallized from methanol: 88 mg, yield = 89%; ^{1}H NMR (400 MHz, CDCl$_3$) δ 9.02 (2H, d, J = 8 Hz), 8.40 (2H, t, J = 8 Hz), 7.98 (2H, d, J = 8.8 Hz), 7.80 (2H, d, J = 8.4 Hz), 7.74−7.59 (10H, m), 7.49−7.46 (6H, m), 7.36 (2H, s), 5.55 (4H, s), 1.47 (6H, s), 1.29 (12H, s); MS m/z (ESI POS) 887.317 {Cu(bpy(Mes)$_2$)(Phdbp)}$^+$. Anal. Calcd for C$_{60}$H$_{48}$N$_4$CuBF$_4$: C, 73.88; H, 4.96; N, 5.75. Found: C, 73.52; H, 5.03; N, 5.69.

Physical Measurements. FT-Raman spectra were obtained using a Bruker Equinox 55 interferometer coupled with a FRA-106 Raman module and a D418T liquid-nitrogen-cooled germanium detector, controlled by the Bruker OPUS v5.5 software package. A Nd:YAG laser operating at 1064 nm and 50 mW of power was used. The spectra were acquired with a resolution of 4 cm^{-1}.

^{1}H NMR spectra of CDCl$_3$ solutions were recorded on a Varian 400 MHz spectrometer at room temperature. All spectra were referenced to the residual CHCl$_3$ peak at 7.26 ppm. Mass spectra were acquired using a Micromass LCT instrument for electrospray measurement or a Shimadzu QP8000 α with an electrospray ionization (ESI) probe. Microanalyses were carried out at the Campbell Microanalysis Laboratory at the University of Otago.

Resonance Raman experiments were performed using a variety of laser sources: for excitation at 350.7, 354.6, 406, and 413 nm, a krypton ion laser (Innova I-302, Coherent Inc.) was used; for excitation at 363.8, 457.9, 488, and 514.5 nm, an argon ion laser (Innova Sabre, Coherent Inc.) was used; for 448.0 nm, a solid-state diode laser (CrystaLaser) was used. Typically, laser intensity at the sample was 25 mW with a beam diameter of approximately 300 μm. The incident beam and the collection lens were arranged in a 135° backscattering geometry to reduce Raman intensity loss by self-absorption.[42] An aperture matched lens was used to focus scattered light through a narrow-band-pass filter (Ruggate), to remove the Rayleigh scattering, and through a quartz wedge (Spex), to remove polarization bias, and onto the 50 μm entrance slit of a spectrograph (Acton Research SpectraPro 500i). The collected light was dispersed in the horizontal plane by a 1200 grooves/mm ruled diffraction grating (blaze wavelength 500 nm) and detected by a liquid nitrogen cooled, back-illuminated Spec-10:100B CCD controlled by a ST-133 controller and WinSpec/32 (version 2.5.8.1) software (Roper Scientific, Princeton Instruments).[43−47] Wavenumber calibration was performed using Raman bands from a 1:1 v/v toluene/acetonitrile sample. Peak positions were reproducible to within 1−2 cm^{-1}. Spectra were obtained with a resolution of 5 cm^{-1}.[48,49] Freshly prepared samples were held in a spinning NMR tube. Typically concentrations were 1 mmol L^{-1} in CH$_2$Cl$_2$.

Argon purged, spectroscopic grade solvents were used for all spectroscopic measurements. Spectral data were analyzed using GRAMS/AI 8.00 (Thermo Electron Corp.) and OriginPro 7.5 (OriginLab Corp.).

Computational Methods. Calculations to determine geometry, vibrational spectra, and electronic spectra were performed using density functional theory with the B3LYP functional[50,51] and the 6-31G(d) basis set.[52] A LANL2DZ core potential[53] was used to model the copper atoms.[45,54,55] All calculations were carried out using the Gaussian 09 software package.[56] For theoretical Raman vibrational energies a scale factor of approximately 0.97 was used; this was found

by minimizing mean absolute deviation (MAD) in the Raman shift between calculated and experimental bands.[57−59] Intensity correction for calculated spectra was applied to convert the Raman activity given by the Gaussian 09 program to Raman scattering cross sections.[60−62] For the jth mode the differential Raman cross section ($\partial\sigma_j/\partial\Omega$) is directly proportional to the observed band intensity. This is related to the Raman activity, S_j, given by the Gaussian 09 frequency calculation (Gaussian Keyword: Freq=Raman) as follows:

$$\frac{\partial\sigma_j}{\partial\Omega} = \left(\frac{2^4\pi^4}{45}\right)\left(\frac{(\nu_0 - \nu_j)^4}{1 - \exp\left[\frac{-hc\nu_j}{kT}\right]}\right)\left(\frac{h}{8\pi^2 c\nu_j}\right)S_j$$

where ν_0 is the laser excitation frequency and ν_j is the frequency of the jth mode.

X-ray Crystallography. X-ray crystal structure measurements were made with a Bruker diffractometer equipped with an Apex II charge-coupled device (CCD) area detector using graphite-mono-chromated Mo Kα ($\lambda = 0.710\,73$ Å) radiation. The structures were solved by direct methods and refined on F^2 by use of all data in full-matrix least-squares procedures. All non-hydrogen atoms were refined anisotropically.

■ RESULTS AND DISCUSSION

Synthesis and Characterization. All complexes were synthesized using the same methodology. One equivalent of [Cu(CH$_3$CN)$_4$]BF$_4$ was added to a solution of bpy(Mes)$_2$ in CH$_2$Cl$_2$ at room temperature, and the solution subsequently turned yellow due to the formation of [Cu(bpy(Mes)$_2$)-(CH$_3$CN)$_2$]$^+$. The second diimine ligand was then added to the mixture; the bpy- and phen-based ligands resulted in red solutions, while the biquinoline-based ligands gave purple solutions. These solutions were then reduced to dryness and the impure solids subsequently recrystallized. Samples were either purified by recrystallization from methanol or by ether diffusion into a dichloromethane solution of the complexes; in some cases, the solvate of the complexes was obtained. All of the complexes presented are air-stable solids and appear to be stable in solution for weeks.

The ^{1}H NMR spectra of the complexes provides an effective diagnostic peak due to the formation of the desired heteroleptic complexes over the formation of any undesired homoleptic complexes. This is the singlet due to the mesityl ring meta aromatic proton that appears between 5.55 and 6.33 ppm in the complexes reported. Upfield shifts of this nature, relative to the free ligand (6.98 ppm), are unusual for aromatic protons and are due to the shielding of aromatic protons by the π system of the second diimine ligand.

Structural Studies. Solid-state structural studies by X-ray crystallography were performed on all but one of the complexes prepared. The crystallographic data and structural refinement data for the complexes are shown in the Supporting Information (Table S1). For many of the complexes, large crystals with dimensions tens of millimeters long were able to be grown, from either slow evaporation from MeOH or CHCl$_3$ or ether diffusion into a concentrated dichloromethane solution of the complexes. Features of some of the structures include intramolecular π stacking between the diimine ligand and a single mesityl ring and severe deviation from perfect tetrahedral geometry. A quantitative method of characterizing four-coordinate geometries is the τ_4 geometry index proposed by Houser.[63] This uses the formula $\tau_4 = \{360° − (\theta − \varphi)\}/141°$, where θ and φ are the two largest angles in the four coordinate geometry. The τ_4 value of a perfect tetrahedron is 1.00 (largest

angles of 109.5°), 0 for square planar (largest angles of 180°), and 0.85 for a perfect trigonal pyramidal (largest angles of 120°), and intermediate geometries fall within the range of 0−1.00. The τ_4 index is used to quantify the effects of the different ligands on the intramolecular π-stacking with the mesityl ring of the bpy(Mes)$_2$ ligand and also the distortion of the Cu(I) ion from a perfect tetrahedral geometry. The τ_4 value for typical Cu(I) bisdiimine complexes such as [Cu(dmp)$_2$]$^+$ and [Cu(6,6′-dimethylbipyridine)$_2$]$^+$ are around 0.75. N−Cu−N angles in these complexes range from ≈125° to around 85°, the latter being found in the five-membered chelate rings.

The crystal structures of [Cu(bpy(Mes)$_2$)(phen)]BF$_4$ and [Cu(bpy(Mes)$_2$)(dmp)]BF$_4$ are shown in Figure 3. The
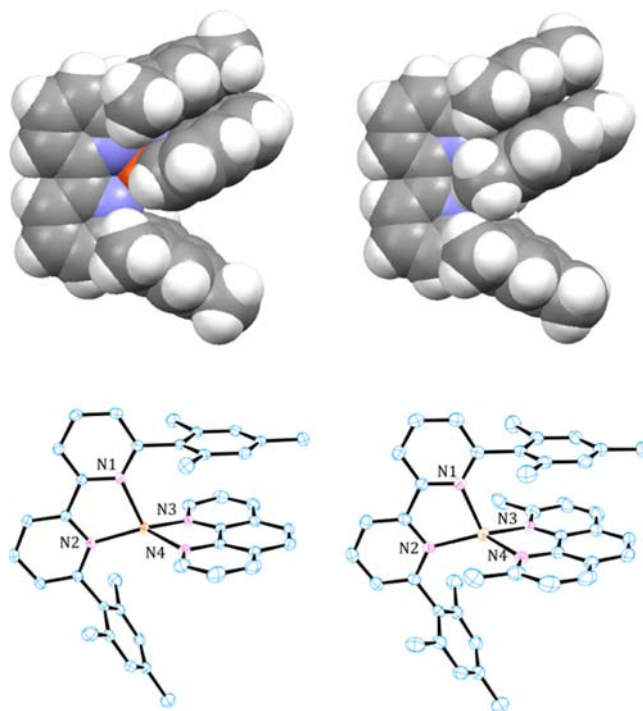
Figure 3. Space-filling diagrams (top) and ORTEP[64] diagrams of [Cu(bpy(Mes)$_2$)(phen)]BF$_4$, [Cu(bpy(Mes)$_2$)dmp)]BF$_4$. Ellipsoids are drawn at the 50% probability level and hydrogen atoms are omitted for clarity in the ORTEP diagrams.

tetrafluoroborate anions are not shown. Both complexes crystallize in the $P2_1/c$ space group and display intramolecular π−π stacking interactions between the phen or dmp ligand and one of the mesityl rings of the bpy(Mes)$_2$ ligand. The distance between the centroid of the π-stacking mesityl ring and the plane of the phen ligand is 3.32 Å for both structures; these distances are well within the ranges for π-stacking.[65] This type of intramolecular π-stacking has also been observed in similar heteroleptic Cu(I) complexes incorporating dipyridophenazine ligands.[26,38]

The similarities between these two structures are borne out by the τ_4 geometry parameter, as shown in Table 1. τ_4 values of 0.667 and 0.656 for [Cu(bpy(Mes)$_2$)(phen)]BF$_4$ and [Cu-(bpy(Mes)$_2$)(dmp)]BF$_4$, respectively, classify the solid-state geometry as distorted trigonal pyramidal. The ^{1}H NMR (vide supra) and UV−vis absorption data (vide infra) are consistent with the complexes adopting the expected tetrahedral Cu(I) geometry in the solution phase, and presumably, the phen ligand is therefore either located more centrally between the

Table 1. Largest N−Cu−N Bond Angles and τ_4 Geometry Parameter for Phenanthroline-Based Complexes

	[Cu(bpy(Mes)₂)(phen)]BF₄	[Cu(bpy(Mes)₂)(dmp)]BF₄
largest angles	N(2)−Cu(1)−N(4) = 127.11°	N(2)−Cu(1)−N(3) = 140.00°
	N(2)−Cu(1)−N(3) = 138.81°	N(2)−Cu(1)−N(4) = 127.38°
τ_4	0.667	0.656

mesityl rings or oscillates back and forth rapidly between each mesityl ring. Presumably, if the π-stacking persisted in solution, the ¹H NMR spectra would display two sets of signals for the mesityl protons. However, only one set of mesityl protons is observed.

The two complexes are also very similar in terms of their intermolecular stacking. The intramolecular π-stacking between the phen ligands and the mesityl ring creates a "void" between the phen ligand and the non-π-stacked mesityl ring, in effect a "Pac-Man"-like semblance. This void is filled by an aromatic portion of an adjacent cation, as shown below in Figure 4. In
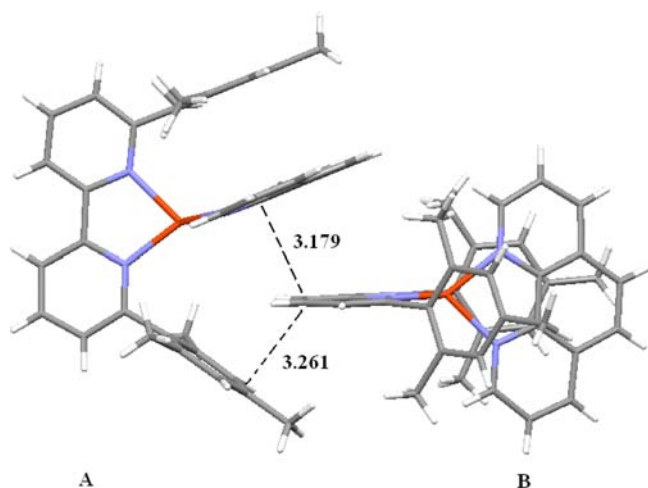

Figure 4. Intermolecular π-interactions of [Cu(bpy(Mes)₂)(phen)]-BF₄, showing the shortest distance between carbon atoms in angstroms.

addition, there are intermolecular interactions between the bpy moiety of the adjacent bpy(Mes)₂ ligand (labeled B in Figure 4) and the phen ligand and mesityl ring of the complex A. We believe the Pac-Man-like structure is due to the creation of the void between the phen ligand and mesityl ring, which is a result of the intramolecular π-stacking. Consistent with this, the crystal structure of [Cu(dpp)₂]⁺ (dpp = 2,9-diphenyl-1,10-phenanthroline) does not show this Pac-Man-like motif because this structure does not possess the requisite intramolecular stacking to engineer the void space.[66] This interaction is seen in the [Cu(bpy(Mes)₂)(phen)]BF₄, [Cu-(bpy(Mes)₂)(dmp)]BF₄, and also previously reported [Cu(bpy(Mes)₂)(dipyridophenazine)]BF₄ structure.[38] In addition, McMillin,[66−68] White,[69,70] and Karpishin[71−74] describe Pac-Man-like distortion of [Cu(NN)₂]⁺ complexes as a rocking distortion.

The structures of the three bpy-based complexes [Cu(bpy-(Mes)₂)(bpy)]BF₄, [Cu(bpy(Mes)₂)(Me₂bpy)]BF₄, and [Cu-(bpy(Mes)₂)(Br₂bpy)] are shown in Figure 5. One difference in these structures compared to the phen-based complexes discussed above is the less pronounced intramolecular π-

stacking between the bpy ligand and a single mesityl ring of the bpy(Mes)₂ ligand. This is particularly evident in both [Cu(bpy(Mes)₂)(Br₂bpy)]BF₄ and [Cu(bpy(Mes)₂)(bpy)]-BF₄, where the bpy ligands sit more centrally between the two mesityl rings, and the mesityl rings "clamp down" on the bpy ligand.

A result of this is that [Cu(bpy(Mes)₂)(Br₂bpy)]BF₄ and [Cu(bpy(Mes)₂)(bpy)]BF₄ do not exhibit any Pac-Man-like intramolecular interactions, as the bpy ligand sits more evenly between the two mesityl rings. The methyl-substituted ligand does show a slight Pac-Man effect. The clamping effect of the mesityl rings is shown by the contracted N1−C1−C11 bond angle of the sp² hybridized carbon (Figure 5) of 113°−115° in the bromo and bpy complexes, compared to angles of 118°−120° in the phen complexes (Table 2). The differences in π-interactions are probably due to the smaller π-system and greater flexibility of the bipyridine ligands compared to the phenanthroline moieties present in the phen-type complexes described above. The differences in the bpy-type complex structures are reflected in the variation in τ_4 (ranging from 0.665 to 0.720); this is much greater than those observed in the corresponding phen-type complexes. The τ_4 of the bpy-type complexes indicates severe distortion from a tetrahedral geometry normally associated with four-coordinate Cu(I) complexes. The solid-state geometry is better described as distorted trigonal pyramidal.

The crystal structures of the biquinoline-based complexes are shown in Figure 6. First, [Cu(bpy(Mes)₂)(biq)]BF₄, which crystallizes in the orthorhombic space group P2₁2₁2₁, with four cations and four tetrafluoroborate anions in the unit cell. This structure is similar to the bpy-based structures in the respect that the mesityl rings clamp down onto the biq ligand via π-interactions. The N1−C1−C11 and N2−C10−C20 bond angles of the sp²-hybridized carbon are 116° and 115°, respectively, slightly less contracted than the bpy compounds (vide supra). The structure is twisted in such a way that one mesityl ring (the "top" ring containing C11, as viewed in Figure 6) is closely associated with one quinoline half of the ligand (N3 quinoline), while the other or "bottom" mesityl ring, containing C20, is closely associated with the other quinoline half (N4) of the biquinoline ligand. The biquinoline ligand is twisted 19° around the C37−C38 bond (the bond that links the two quinoline moieties, the N−C−C−N torsion angle), and the bpy(Mes)₂ ligand is twisted 10° around the C5−C6 bond to accommodate this pairing up of quinoline and mesityl moieties. This can be contrasted with the [Cu(biq)₂]BF₄ crystal structure, where the biquinoline ligands are orthogonal to each other and each biquinoline ligand is almost planar with the respective N−C−C−N dihedral angle less than 1°.[75] The extent of twisting in biquinoline ligand is also greater than observed in the bpy type complexes, where the N−C−C−N torsion angles range from 2° to 5°. Planes through the mesityl rings are at a 7° angle to their respective quinoline half, with centroid to centroid distances of 3.68 and 3.76 Å for the C11 mesityl to N4 pyridyl and C20 mesityl to N3 pyridyl rings, respectively.

[Cu(bpy(Mes)₂)(Phdbq)]BF₄ crystallizes in the monoclinic space group P2₁/c with four cations and four tetrafluoroborate anions in each unit cell. The Phdbq ligand structure differs from the biquinoline structure due to the 3,3′-dimethylene bridge linking the two quinoline moieties, as well as the two phenyl rings at the 4,4′-position. The Phdbq ligand is less twisted than the biq ligand, with a N−C−C−N dihedral angle of 14°, the
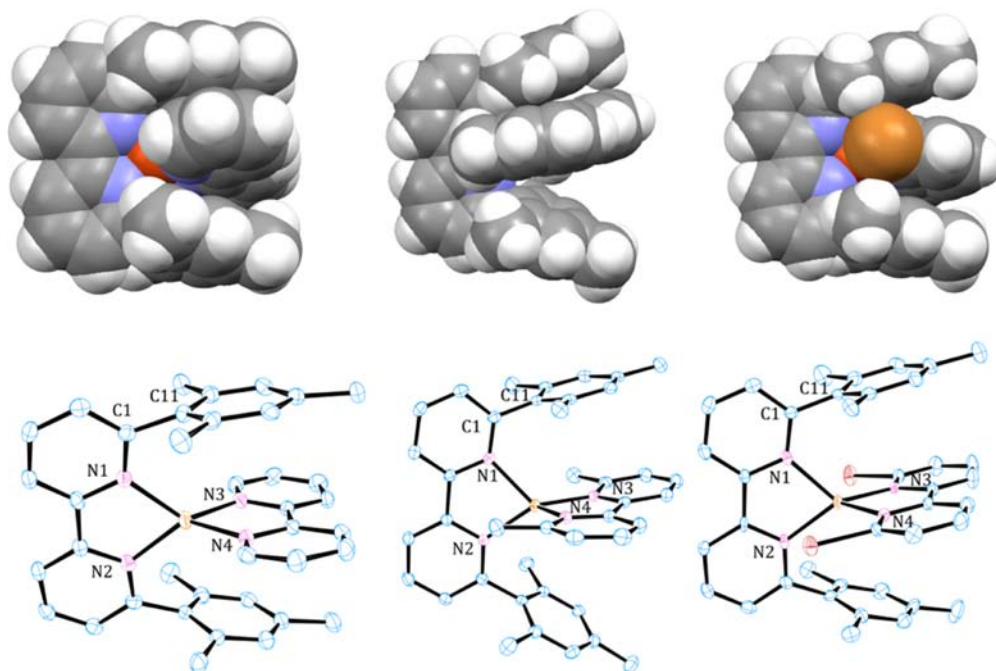
2984

dx.doi.org/10.1021/ic302393p | Inorg. Chem. 2013, 52, 2980−2992

Figure 5. Space-filling diagrams (top) and ORTEP[64] diagrams with ellipsoids at the 50% probability level for $[Cu(bpy(Mes)_2)(bpy)]BF_4$, $[Cu(bpy(Mes)_2)(Me_2bpy)]BF_4$, and $[Cu(bpy(Mes)_2)(Br_2bpy)]BF_4$, respectively.

Table 2. Largest N−Cu−N Bond Angles and τ_4 Geometry Parameter for the Bipyridine-Based Complexes

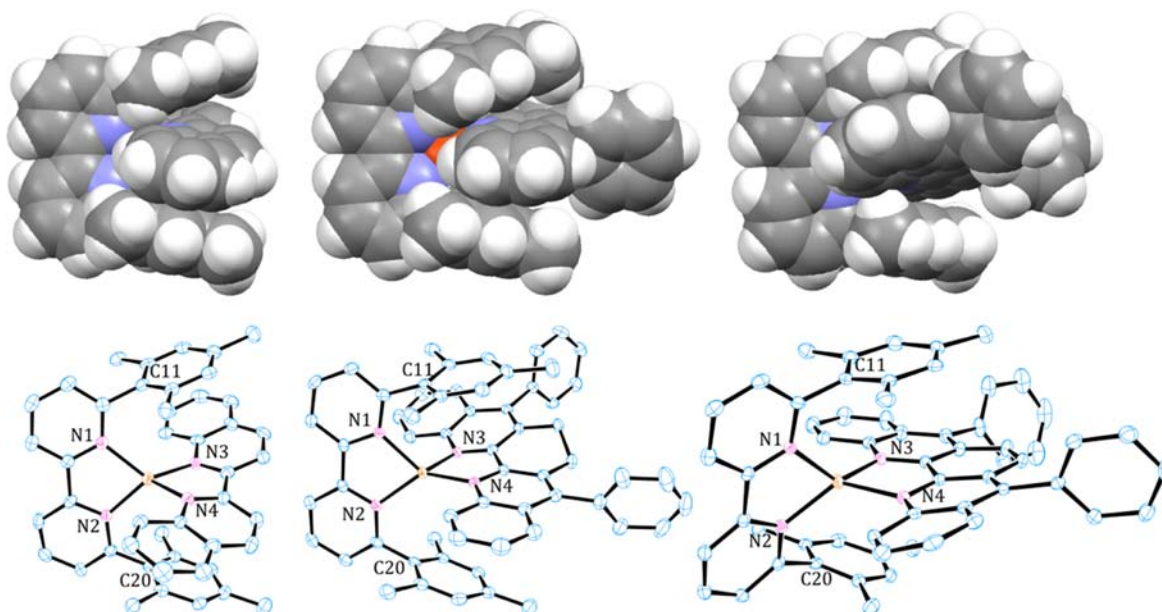|	$[Cu(bpy(Mes)_2)(bpy)]BF_4$	$[Cu(bpy(Mes)_2)(Me_2bpy)]BF_4$	$[Cu(bpy(Mes)_2)(Br_2bpy)]BF_4$
largest Angles	N(3)−Cu(1)−N(1) = 131.6°	N(3)−Cu(1)−N(2) = 142.31°	N(3)−Cu(1)−N(2) = 136.24°
	N(2)−Cu(1)−N(4) = 129.88°	N(3)−Cu(1)−N(1) = 124.27°	N(3)−Cu(1)−N(1) = 127.13°
τ_4	0.698	0.665	0.720

Figure 6. Space-filling diagrams (top) and ORTEP[64] diagrams with ellipsoids at the 50% probability level for $[Cu(bpy(Mes)_2)(biq)]BF_4$, $[Cu(bpy(Mes)_2)(Phdbq)]BF_4$, and $[Cu(bpy(Mes)_2)(Phdbp)]BF_4$, respectively.

dimethylene bridge restricting torsion of the ligand. The mesityl rings interact through π-interactions with Phdbq ligand and clamp onto the Phdbq ligand, as indicated with N−C−C angles of 115°. The bpy(Mes)$_2$ ligand is not as twisted as in the case of the biquinoline structure and has a N−C−C−N

dihedral angle of 2°. However, the bpy(Mes)$_2$ and Phdbq ligands are tilted from an ideal orthogonal geometry, with an acute angle between the two coordination geometries of 79°.

The $[Cu(bpyMes)(Phdbp)]BF_4$ crystal structure reflects the planar aromatic nature of the Phdbp ligand. There is still a

Table 3. Largest N−Cu−N Bond Angles and τ_4 Geometry Parameter for Biquinoline-Based Complexes

	$[Cu(bpy(Mes)_2)(biq)]BF_4$	$[Cu(bpy(Mes)_2)(Phdbq)]BF_4$	$[Cu(bpy(Mes)_2)(Phdbp)]BF_4$
largest angles	N(4)−Cu(1)−N(2) = 133.58°	N(4)−Cu(1)−N(2) = 134.61°	N(3)−Cu(1)−N(1) = 133.64°
	N(3)−Cu(1)−N(1) = 128.27°	N(4)−Cu(1)−N(1) = 131.97°	N(3)−Cu(1)−N(2) = 129.56°
τ_4	0.696	0.663	0.687

slight twisting of the ligand though with the N−C−C−N dihedral angle of 9°. This is much flatter than the Phdbq and biq ligands, which have angles of 14° and 19°, respectively. The mesityl rings clamp down on the Phdpb ligand with clamping angles of 114° and 115°. The Phdbp and bpy(Mes)$_2$ ligands are not orthogonal to each other, with an acute angle between the two ligand planes of 78° (Figure 6). This tilt results in the C11 mesityl ring lying over the center of the phenanthroline moiety, while the C20 mesityl ring is over the N3 quinoline moieties. The plane through the C11 mesityl rings is at 7° to the plane through the atoms of the phenanthroline moiety, while the C20 mesityl ring is less parallel to the phen plane at 22°. The distorted nature of the coordination geometry of the biquinoline-based complexes is reflected in the τ_4 values, given in Table 3. The coordination geometries in the solid state are best described as distorted trigonal pyramidal.

Electrochemistry. The complexes were studied by cyclic voltammetry in dry, nitrogen-purged dichloromethane; the half-wave potentials of the oxidation and reduction (where observed) processes are given in Table 4. Cyclic voltammograms of $[Cu(bpy(Mes)_2)(bpy)]BF_4$, $[Cu(bpy(Mes)_2)(Me_2bpy)]BF_4$, and $[Cu(bpy(Mes)_2)(Br_2bpy)]BF_4$ are shown in Figure 7.

Table 4. Electrochemical Data for the Complexes[a]

	$E_{1/2}$/V vs SCE[b]	$E_{1/2}$/V vs SCE[c]
$[Cu(bpy(Mes)_2)(phen)]BF_4$	0.78	−
$[Cu(bpy(Mes)_2)(dmp)]BF_4$	0.92	−
$[Cu(bpyMes)_2)(bpy)]BF_4$	0.73	−
$[Cu(bpyMes)_2)(Me_2bpy)]BF_4$	0.91	−
$[Cu(bpyMes)_2)(Br_2bpy)]BF_4$	1.06	−
$[Cu(bpyMes)_2)(biq)]BF_4$	0.90	−1.38
$[Cu(bpyMes)_2)(Phdbq)]BF_4$	0.84	−1.49
$[Cu(bpyMes)_2)(Medbq)]BF_4$	0.91	−1.37
$[Cu(bpyMes)_2)(Phdbp)]BF_4$	0.91	−1.29

[a]$E_{1/2}$ recorded relative to DMFc$^+$/DMFc and converted vs SCE. Solvent was CH_2Cl_2, and supporting electrolyte was TBAPF$_6$. [b]Oxidation process. [c]Reduction process.

All complexes exhibited a reversible oxidation wave, which is assigned as the Cu(I) to Cu(II) process. The half-wave oxidation potentials are dependent on the extent of the steric bulk around the Cu(I) center. This is in accordance with the change of preferred geometry as Cu(I) (tetrahedral) is oxidized to Cu(II) (square-planar). The increased steric bulk around the Cu(I) coordination sphere stabilizes the Cu(I) center to oxidation.[73] This is exemplified by comparing the oxidation potentials of $[Cu(phen)_2]^+$ (0.50 V vs SCE) and $[Cu(dmp)_2]^+$ (0.83 V) in dichloromethane solution. The oxidation potentials of the complexes presented here reflect this. The $E_{1/2}$ values observed for the oxidation of the complexes are lower (less positive) when the ligand has no methyl groups or bromine atoms ortho to the coordinating nitrogens, namely, the $[Cu(bpy(Mes)_2)(phen)]BF_4$ and $[Cu(bpy(Mes)_2)(bpy)]BF_4$ complexes.
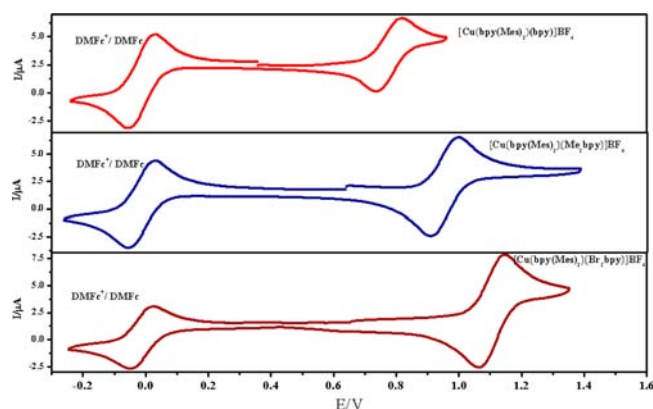

Figure 7. Cyclic voltammograms of the first oxidation of $[Cu(bpy-(Mes)_2)(bpy)]BF_4$, $[Cu(bpy(Mes)_2)(Me_2bpy)]BF_4$, and $[Cu(bpy-(Mes)_2)(Br_2bpy)]BF_4$ with DMFc in solution. Solution concentrations were typically about 10^{-3} M in CH_2Cl_2 with 0.1 M tetrabutylammonium hexafluorophosphate (TBAPF$_6$) added as a supporting electrolyte.

The dmp, Me$_2$bpy, and Br$_2$bpy complexes have the most positive potentials for the oxidation process, owing to the increased steric bulk around the Cu(I) center. The biquinoline-based complexes all have similar oxidation potentials. This is consistent with their similar Cu(I) coordination environments.

The $E_{1/2}$ of the oxidation process of the phen- and bpy-based complexes are comparable to those reported by Odobel and co-workers[26] in a study of the corresponding mesityl-substituted phenanthroline complexes. This suggests that the relative ease of forming square planar Cu(II) is not greatly altered by substitution of the rigid phen(Mes)$_2$ with the more flexible bpy(Mes)$_2$ ligand. This may be somewhat surprising considering the greater flexibility of the bpy(Mes)$_2$ ligand compared to the phenanthroline moiety.

For the phen, dmp, bpy, Me$_2$bpy, and Br$_2$bpy complexes, no reduction was observed within the dichloromethane solvent limit, meaning no ligand-based reduction [or Cu(0) formation] is observed, consistent with previous work on the respective homoleptic complexes.[2] For the complexes where reduction waves are observed, these are assigned as population of the respective biquinoline-based ligand LUMO, consistent with previous literature.[76,77]

Electronic Absorption Spectra and TD-DFT Calculations. The electronic absorption spectra of the phen- and bpy-based complexes are shown in Figure 8, and the corresponding experimental and TD-DFT data are given in Table 5. All of the phen- and bpy-based complexes are red in color. In the visible region, the spectra are dominated by a band around 470 nm. This is assigned as an MLCT transition from the Cu(I) metal center to the bpy/phen ligands(s). Each complex has intense bands in the UV region of the spectrum, due to ligand-based π−π*-transitions.

The energies of the transitions are red-shifted from those of the homoleptic Cu(I) complexes $[Cu(dmp)_2]^+$ (λ_{max}, 455 nm), $[Cu(phen)_2]^+$ (λ_{max}, 435 nm), and $[Cu(Me_2bpy)_2]^+$ (λ_{max}, 455

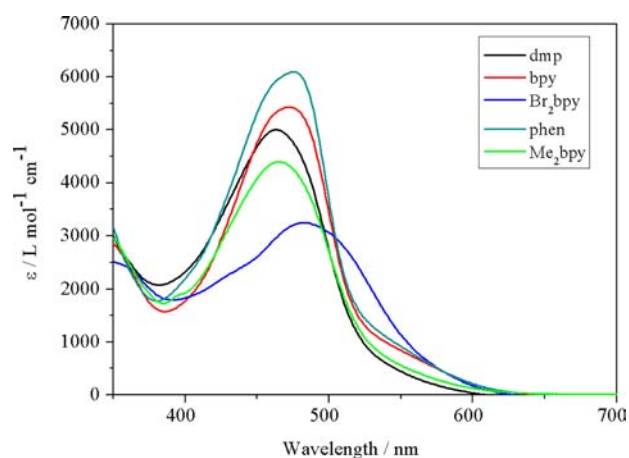**Figure 8.** UV−vis absorption spectra of the phen- and bpy-based $[Cu(bpy(Mes)_2)(NN)]^+$ complexes in CH_2Cl_2 solution.

nm). The lower energies for the MLCT transitions of the heteroleptic $[Cu(bpy(Mes)_2)(NN)]^+$ complexes can be attributed to intramolecular $\pi-\pi$-interactions between the mesityl groups and the phen- and bpy-based ligand. Another factor that determines the energy of the MLCT transition is the steric bulk around the coordination sphere, as has been observed previously.[1,4,27] For example, the energies of the MLCT transition of the phen (λ_{max}, 476 nm) and bpy (λ_{max}, 472 nm) complexes are red-shifted from those of dmp (λ_{max} 463 nm) and Me2bpy (λ_{max} 465 nm) complexes. It should be noted that $[Cu(bpy(Mes)_2)(Br_2bpy)]$ does not fit this pattern; this is because the Br_2bpy ligand has a lower energy π^* MO, resulting in a red-shifted MLCT transition (482 nm). The extinction coefficients of the complexes are typical for the MLCT transition of Cu(I) polypyridyl complexes; the Br_2bpy complex has the smallest (3200 L mol^{-1} cm^{-1}).

Time-dependent density functional theory (TD-DFT) calculations were performed with a dichloromethane solvent field on the geometry obtained from the in-vacuo optimization calculation, using the crystal structure geometries. It is generally found that the shifts in energies are well-predicted, but the absolute values are offset; this is true for charge-transfer transitions, as has been discussed by Dreuw and Head-Gordon.[78] With the exception of the Br_2bpy complex, the predicted energies for the MLCT transition of the phen- and

bpy-based complexes (Table 5) are similar, around 450 nm. The calculation predicts the observed result that the Br_2bpy complex has a lower energy of absorption compared to the other phen- and bpy-based complexes, observed at 482 nm (predicted 476 nm). The nature of this transition appears different from the other phen- and bpy-based complexes. This is supported by the band shapes and extinction coefficients; other than those of $[Cu(bpy(Mes)_2)(Br_2bpy)]BF_4$, the band shapes are similar to those of the respective homoleptic complexes. The spectrum of $[Cu(bpy(Mes)_2)(Br_2bpy)]BF_4$ shows the lowest energy maximum (482 nm), and the band is much broader than those observed in the other spectra. This is indicative of the electron-withdrawing nature of the bromine atoms, which lowers the energy of the Br_2bpy LUMO relative to the $bpy(Mes)_2$ ligand, and hence, the MLCT to the Br_2bpy ligand has greater oscillator strength.

For the other complexes with a bpy- or phen-based diimine ligand, it can be assumed that the energies of the LUMO of the $bpy(Mes)_2$ and the bpy or phen diimine ligand are very similar. This suggests that two MLCT transitions may be possible, each populating orbitals on the two different diimine ligands. However, for example, the TD-DFT calculations for the phen complex suggest an MLCT transition made up of two configurations, HOMO−1→LUMO and HOMO→LUMO+1 (Table 5), in which the LUMO is bpy-based and the LUMO+1 is phen/bpy-based; in essence, this is describing an MLCT transition that is delocalized across both ligands. The existence of delocalized MLCT excited states has been the subject of intense research effort in the past.[79−82] The weight of evidence is that MLCT transitions in homoleptic Cu(I) complexes are localized in solution, and this would certainly be expected for heteroleptic systems.[83−85]

Each of the bpy- and phen-based complexes (except Br_2bpy) has calculated MLCT transitions that terminate on both of the diimine ligands. Resonance Raman spectroscopy is used to gain insight into the nature of these transitions (vide infra).

The UV−vis absorption spectra for the biquinoline-based complexes are shown in Figure 9, with data given in Table 5. The complexes all appear purple in color, with the absorption maxima of the Medbq, Phdbq, and biq complexes at 533, 547, and 541 nm, respectively. The Phdbp complex is dominated by two bands of similar intensity in the visible region, with absorption maxima at 561 and 451 nm.

Table 5. Experimental and Calculated Electronic Data for the Complexes

	experimental		calculated		
compound	λ/nm	ε/L mol^{-1} cm^{-1}	λ/nm	f	MO configurations, major components (coefficient)[a]
$[Cu(bpy(Mes)_2)(phen)]BF_4$	476	6100	450	0.13	H−1, L (0.50); H, L+1 (−0.49)
$[Cu(bpy(Mes)_2)(dmp)]BF_4$	463	5000	452	0.06	H−1, L (0.59); H−1, L+1 (−0.28)
$[Cu(bpy(Mes)_2)(bpy)]BF_4$	472	5400	452	0.11	H−1, L (0.36); H−1, L+1 (0.34)
$[Cu(bpy(Mes)_2)(Me_2bpy)]BF_4$	465	4400	451	0.06	H−1, L (0.21); H, L (0.61); H, L+1 (0.11)
$[Cu(bpy(Mes)_2)(Br_2bpy)]BF_4$	482	3200	476	0.05	H, L (0.88)
$[Cu(bpy(Mes)_2)(biq)]BF_4$	541	3600	507	0.07	H, L (0.80); H−1, L (0.11)
$[Cu(bpy(Mes)_2)(Phdbq)]BF_4$	547	4900	492	0.08	H, L (0.54); H−1, L (0.28)
$[Cu(bpy(Mes)_2)(Medbq)]BF_4$	533	4400	497	0.08	H−1, L (0.23); H, L (0.64)
$[Cu(bpy(Mes)_2)(Phdbp)]BF_4$	561	5200	520	0.11	H, L (0.89)
	451	5000	449	0.08	H, L+1 (0.89)

[a]H = HOMO, L = LUMO.
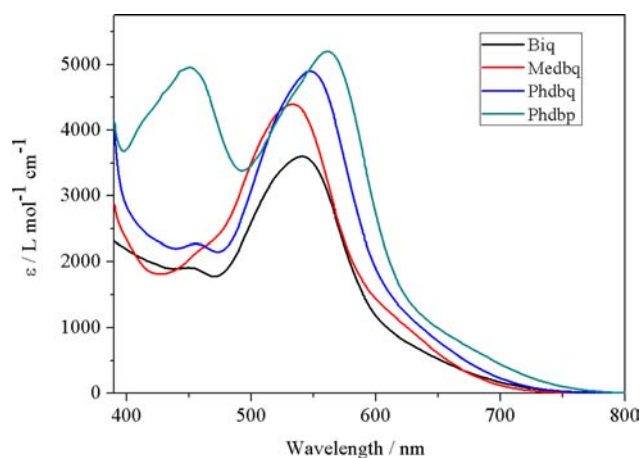
Figure 9. UV−vis absorption spectra of the biquinoline-based [Cu(bpy(Mes)$_2$)(NN)]$^+$ complexes in CH$_2$Cl$_2$ solution.

Figure 10. Comparison between the experimental and calculated FT-Raman spectra of [Cu(bpy(Mes)$_2$)(dmp)]BF$_4$.

The energies of the predicted transitions for [Cu(bpy-(Mes)$_2$)(biq)]BF$_4$ and [Cu(bpy(Mes)$_2$)(Medbq)]BF$_4$ are quite similar, around 500 nm. The nature of the transitions are MLCT from a Cu(I) dπ orbital to the biquinoline-based LUMO. This is to be expected as the biquinoline-based LUMO is much lower in energy than the bipyridine-based LUMO. This presence of a second strong transition in the visible region for [Cu(bpy(Mes)$_2$)(Phdbp)]BF$_4$ is predicted by the TD-DFT calculation. The lowest energy band (observed 561 nm, predicted 520 nm) is assigned as HOMO → LUMO, similar to other biquinoline-based complexes. The second strong transition is more accurately predicted at 449 nm (observed 451 nm) and is assigned as MLCT to Phdbp LUMO+1. The LUMO+1 of Phdbp is low enough energy to be populated in the visible region due to the extended aromatic system of the ligand. The extended aromatic system of the Phdbp ligand results in the low energy LUMO+1 being populated by an MLCT transition in the visible region.

Normal and Resonance Raman Spectroscopy. The frequencies and intensities of Raman bands can be calculated in order to simulate a normal Raman spectrum, which can be compared to the experimental data. The goodness-of-fit between the experimental and calculated Raman data may be parametrized by the mean-absolute deviation (MAD), in order to determine the accuracy of calculations.[86−89] Calculated spectra can then be used to assign the bands, which is important for identifying the enhanced vibrational models in the resonance Raman spectra.

Figure 10 shows the calculated and experimental FT-Raman spectra of [Cu(bpy(Mes)$_2$)(dmp)]BF$_4$; this has a MAD of 5 cm^{-1} on the basis of comparing the experimental values that are greater than 20% of the maximum observed intensity. The MADs for the other complexes range from 5 to 10 cm^{-1}. This is considered a good correlation.[57] Although the calculated vibrational spectra for the data result in satisfactory MADs, for some of the complexes studied here an unambiguous assignment of all vibrational modes is not always possible because the transitions overlap. However, for each compound a sufficient number of unambiguous assignments could be made to characterize the Franck−Condon state.

For the normal Raman spectra of the complexes, a series of bands at similar frequencies are apparent for all the complexes, 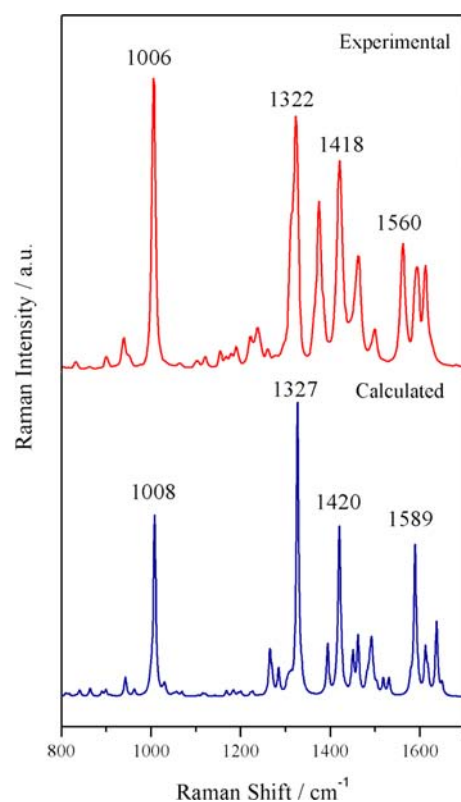and these bands are assigned to the bpy(Mes)$_2$ ligand. The most prominent of these lie at approximately 1005, 1325, and 1560 cm^{-1}.

Resonance Raman spectroscopy can be used to elucidate the structural changes upon excitation into the initially populated Franck−Condon state. This is possible as the enhancements observed in resonance Raman spectra, compared to the normal Raman spectra, are not random but specific to the modes of vibration that mimic the structural distortion upon excitation.[90,91] Hence vibrational modes that are enhanced are associated with the active chromophore. For the complexes where the energy of the LUMOs on each ligand are close in energy to each other and, hence, MLCT transition may populate either/or both of the diimine ligands, the resonance Raman spectra can elucidate which ligand is being populated in the FC state. Of course, in addition to the structural distortion (Δs) other factors can affect the resonance Raman scattering cross section.[45,55] Thus, it is possible that in these systems in which there are heteroleptic ligands that one ligand may be a much better Raman scatterer than the other and thus may contribute more strongly to the observed spectrum.

As will be shown, the resonance Raman spectra and TD-DFT results for the purple, biquinoline-based complexes are much more straightforward to assign and interpret, as the dominant transition is the MLCT which populates the LUMO of the biquinoline-type ligand. The TD-DFT data for the complexes predict the electronic transitions of the purple compounds as populating the LUMO of the biquinoline-type ligand.

The resonance Raman spectra of [Cu(bpy(Mes)$_2$)(dmp)]-BF$_4$ at a variety of excitation wavelengths are shown in Figure 11. The dmp complex shows enhancements of bands at 1374, 1464 1560, and 1593 cm^{-1} across the wavelengths 406−488
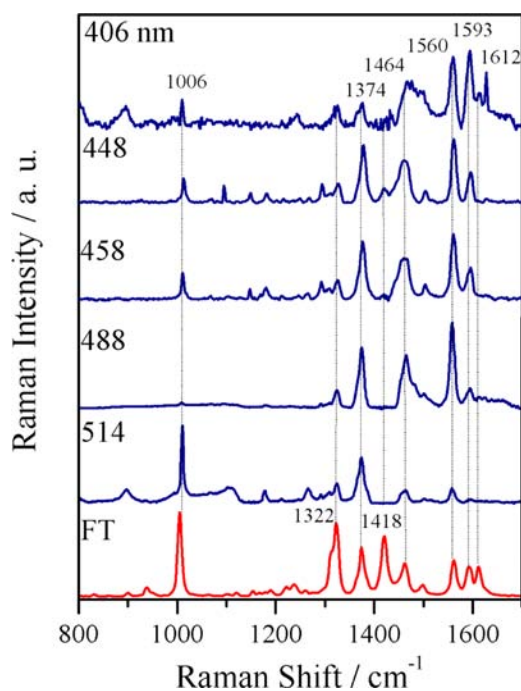
nm. These bands are all modes located on the bpy(Mes)$_2$ ligand.

Figure 11. Resonance Raman spectra (blue) of [Cu(bpy(Mes)$_2$)-(dmp)]BF$_4$ in CH$_2$Cl$_2$ at a range of excitation wavelengths. The solution concentration was approximately 10^{-3} mol L^{-1}. FT-Raman spectra (red) of powder sample acquired at 1064 nm.

Bands at 1418 and 1612 cm^{-1} are both vibrations based on the dmp ligand and are not relatively enhanced across the same wavelengths. Interestingly, the band around 1320 cm^{-1}, which is enhanced in the bpy-based compounds, is not enhanced in the dmp spectra. The calculated vibrational mode for this vibration predicts a delocalized vibration involving both ligands. Excitation with 514 nm wavelength enhances the bpy-based band at 1006 cm^{-1}; this wavelength is probing the shoulder of the MLCT band.

The shoulder of the MLCT band is assigned as a transition with torsion between the two ligand planes, deviating from D_{2d} symmetry.[33,92] The enhancement of this particular bpy-based band at ca. 1006 cm^{-1} is observed not only for [Cu(bpy-(Mes)$_2$)(dmp)]BF$_4$ (Figure 11), but also [Cu(bpy(Mes)$_2$)-(bpy)]BF$_4$ (Figure S1, Supporting Information), and [Cu(bpy-(Mes)$_2$)(phen)]BF$_4$ (Figure S2, Supporting Information). One plausible explanation for this enhancement pattern is that the 1006 cm^{-1} band possesses a degree of torsional character that selectively enhances it for the lower energy transition. This is not inconsistent with the experimental data, but careful analysis of the calculated mode does not provide unequivocal support for this explanation. In the UV−vis spectra the lowest energy transition (often referred to as band I) appears as a shoulder on the main MLCT. In all cases in the DFT calculations this is a HOMO→LUMO transition, thus having a similar orbital parentage to the much more intense band II features (Table 5). In this sense, the DFT calculations do not appear to provide decisive insight into this part of the optical spectrum.

The TD-DFT calculations predict the dominant configuration of the MLCT transition being HOMO−1 to LUMO (59%), where the LUMO occupies the bpy moiety of the

bpy(Mes)$_2$ ligand, which is consistent with the enhancement of bpy bands over dmp bands. The resonance Raman spectra of [Cu(bpy(Mes)$_2$)(Br$_2$bpy)]BF$_4$ (Figure S1, Supporting Information) across the same excitation wavelengths show similar features to the dmp complex, that is, enhancement of bands assigned as bpy(Mes)$_2$ ligand vibrations.

The enhancement of bands due to the bpy(Mes)$_2$ ligand in preference to the Br$_2$bpy ligand is somewhat surprising given the energy and band-shape of the MLCT band in the absorption spectrum of [Cu(bpy(Mes)$_2$)(Br$_2$bpy)]BF$_4$, which suggests that the chromophore is dominated by the Br$_2$bpy ligand. The TD-DFT calculation also predicts the dominant MLCT transition being that involving the Br$_2$bpy ligand.

The resonance Raman spectra of [Cu(bpy(Mes)$_2$)-(Me$_2$bpy)]BF$_4$ show two distinct patterns of enhancements across the excitation wavelengths used (Figure 12). Excitation
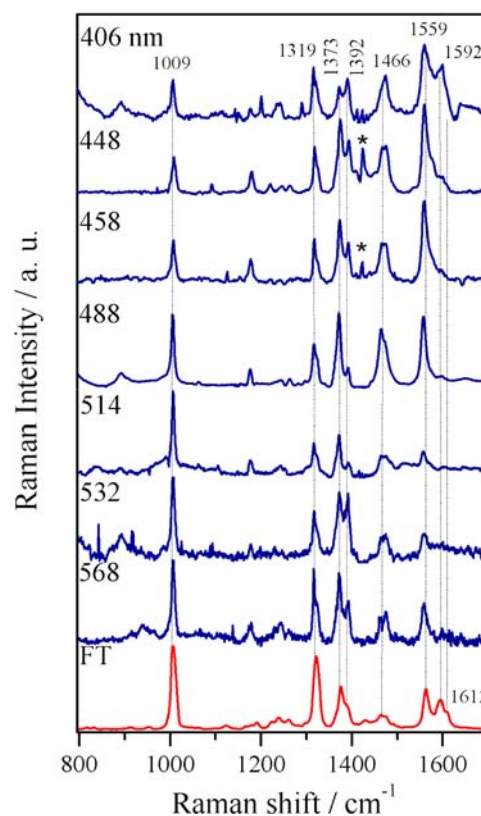

Figure 12. Resonance Raman spectra (blue) of [Cu(bpy(Mes)$_2$)-(Me$_2$bpy)]BF$_4$ in CH$_2$Cl$_2$ at a range of excitation wavelengths. The solution concentration was approximately 10^{-3} mol L^{-1}. FT-Raman spectra (red) of powder sample acquired at 1064 nm. Solvent bands are marked (*).

wavelengths from 406 to 488 nm show bands enhanced at 1009, 1319, 1373, 1466, and 1559 cm^{-1}. Excitation wavelengths from 514 to 568 show enhancement of some of the same bands that are enhanced across 406−488 nm (1009, 1319, and 1373 cm^{-1}) but diminution of the 1466 and 1559 cm^{-1} bands.

The bands at 1009, 1373, and 1559 cm^{-1} are bpy bands of the bpy(Mes)$_2$ ligand, and the 1466 cm^{-1} band is a Me$_2$bpy band. Assignment of the 1319 cm^{-1} band is ambiguous, as two calculated modes similar in calculated energy and intensity lie at 1303 and 1309 cm^{-1}, but these are the same bpy-based stretching modes, but localized on the bpy(Mes)$_2$ and bpy ligands, respectively.

The same stretching modes on the two bpy-based ligands are expected to have similar frequencies of vibration and, in this complex, may in fact occur at the same energy. The enhancement of bands due to both ligands indicates that both ligands are involved in the MLCT chromophore. One interpretation of the data is that the FC state of the molecule is delocalized over both ligands. However, the FC state of $[Cu(I)(diimine)_2]^+$ polypyridyls is known to be localized on one of the diimine ligands. A more likely explanation is that, as the energy levels of the MLCT transitions to each of the ligands is very similar, in solution there exists a population of molecules where the FC state is localized on the $bpy(Mes)_2$ ligand and also a population of molecules where the FC state is localized on the Me_2bpy ligand. TD-DFT calculations predict LUMOs of similar energy. The band at 1612 cm^{-1} in the FT spectrum, which is not enhanced with excitation of any of the wavelengths used, is assigned as a stretching mode of the mesityl rings of the $bpy(Mes)_2$ ligand. This is consistent with the MLCT to the $bpy(Mes)_2$ ligand not having a lot of wave function amplitude on the mesityl substituent.

The resonance Raman spectra of $[Cu(bpy(Mes)_2)(bpy)]BF_4$ and $[Cu(bpy(Mes)_2)(phen)]BF_4$ (Figures S1 and S2, Supporting Information) show very similar features to that of $[Cu(bpy(Mes)_2)(Me_2bpy)]$, with enhancement of bands due to both ligands, indicating MLCT transitions that populate each ligand. This is also consistent with the TD-DFT calculations that predict the LUMO orbitals localized on each ligand to be close in energy to each other and both involved in the electronic transition (Table 5).

The resonance Raman spectra of the purple, biquinoline-based complexes are much more straightforward than those of the bpy- and phen-based complexes. The enhancement patterns for all the purple complexes show selective enhancement of vibrational modes of the biquinoline-based ligand over the $bpy(Mes)_2$ ligand. This is consistent with the lower energy of the MLCT absorption in the visible spectra of the biquinoline complexes. The resonance Raman spectra of $[Cu(bpy(Mes)_2)(Medbq)BF_4$ in Figure 13 is an example, and the spectra for the other biquinoline-based complexes are shown in the Supporting Information (Figures S4–S6). Three bands are drastically enhanced over the wavelengths examined, those being at 1379, 1458, and 1550 cm^{-1}. These are all vibrations of the Mebdq ligand. Diminution of bands at 1010 and 1323 cm^{-1} compared to the FT-spectrum, which are bpy-based bands, is also consistent with the dominant chromophore being the Cu(I) to Medbq MLCT transition.

To summarize, the resonance Raman spectra of the purple, biquinoline-based complexes all show enhancement of bands due to vibrational modes localized on the biquinoline-type ligand. Therefore, the dominant chromophore is the MLCT transition that populates the biquinoline-type ligand rather than the $bpy(Mes)_2$ ligand. The resonance Raman spectra $[Cu(bpy(Mes)_2)(Me_2bpy)]BF_4$, $[Cu(bpy(Mes)_2)(bpy)]BF_4$, and $[Cu(bpy(Mes)_2)(phen)]BF_4$ show enhancement of both $bpy(Mes)_2$ modes, and the second diimine ligand. This indicates that the MLCT transitions to each ligand are close in energy to each other and population of each localized FC state occurs.

Photophysical Properties. Many Cu(I) diimine complexes are emissive from a long-lived triplet excited state in solution. Cu(I) diimine complexes with bulky substituents around the Cu center, which protect the excited state from deactivation from solvent molecules, are typically emissive. For this reason, one might expect the complexes with bulky groups
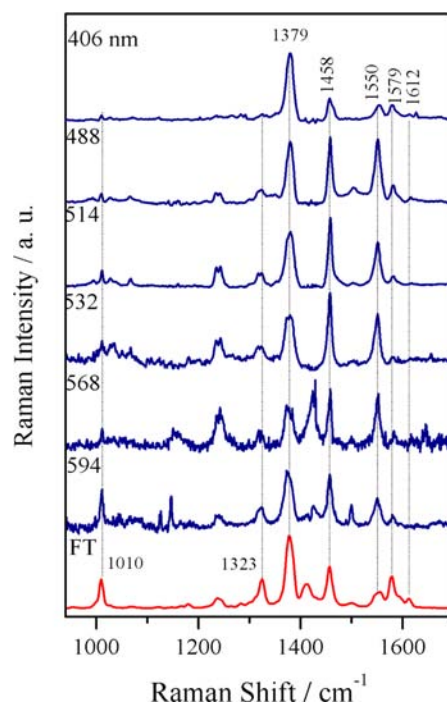

Figure 13. Resonance Raman spectra of $[Cu(bpy(Mes)_2)(Medbq)]BF_4$ in CH_2Cl_2 at a range of excitation wavelengths. The solution concentration was approximately 10^{-3} mol L^{-1}. FT-Raman spectra of powder sample acquired at 1064 nm.

presented in this study, $[Cu(bpy(Mes)_2)(dmp)]BF_4$, $[Cu(bpy-(Mes)_2)(Me_2bpy)]BF_4$, and $[Cu(bpy(Mes)_2)(Br_2bpy)]BF_4$, to be emissive in solution. For these complexes we observe only weak emission. Attempts to study the transient absorption of the complexes were unsuccessful, as degassed solutions of the complexes degraded immediately following irradiation with a 355 nm laser pulse, implying that any excited state is short-lived ($\tau < 5$ ns)

The weakly emissive nature of the heteroleptic complexes in this study is in contrast to the findings of Odobel and co-workers,[26] where all but one of the complexes they studied were found to be emissive in dichloromethane solution. The complexes presented by Odobel and co-workers were found to be emissive in acetonitrile, a solvent known to deactivate excited states. However, other researchers have noted that bpy-based ligands give short τ for Cu(I) complexes.[93,94] The oxidation potentials of the complexes presented here and those of the complexes studied by Odobel and co-workers are comparable, meaning the steric constraint around the Cu(I) center is similar in both types of complexes. The increase of steric bulk around the Cu(I) center has previously been used to improve the emissive properties of the complexes. One possible explanation for the nonemissive nature of the $bpy(Mes)_2$-based complexes is that, compared to the phenanthroline-based complexes reported by Odobel and co-workers, the bpy complexes are much more flexible than the phen-based systems. This greater flexibility may result in photodisassociation of the complexes, rather than sustaining the flattened triplet state responsible for long-lived emission. In the case of homoleptic-biquinoline-based Cu(I), weak emission has been observed at low temperatures.[77] However, strong emission is observed when a benzoquinoline motif is used, creating a highly crowded Cu(I) coordination sphere.[95]

■ CONCLUSIONS

In this paper, we report the synthesis of nine heteroleptic Cu(I) complexes, with bpy(Mes)$_2$ and nine diimine ligands, using the HETPEHN strategy. Eight of the complexes are characterized by X-ray crystallography. The Cu(I) four-coordinate geometries are quantified using the τ_4 parameter. The phen-based complexes exhibit stacking between the phen ligand and one of the mesityl rings, creating a Pac-Man motif. On the other hand, the bpy-based complexes show different types of packing interaction, with both mesityl rings "clamping down" on the bpy-based ligand and π-stacking. Cyclic voltammetry is used to examine the oxidation process of the Cu(I) metal center, which indicate the extent of steric bulk around the coordination sphere. The Cu(I) MLCT transitions of the complexes are investigated with resonance Raman spectroscopy in concert with TD-DFT calculations. The resonance Raman spectra of the purple complexes are straightforward, in that vibrational bands of the biquinoline-based ligand are selectively enhanced over bpy(Mes)$_2$ bands. This is consistent with the purple color of the complexes, due to the lower energy of the biquinoline-based LUMO compared to the bpy(Mes)$_2$ LUMO. All the phen- and bpy-based complexes show enhancement of bpy(Mes)$_2$ bands. The resonance Raman spectra of [Cu(bpy-(Mes)$_2$)(bpy)]BF$_4$, [Cu(bpy(Mes)$_2$)(phen)]BF$_4$, and [Cu-(bpy(Mes)$_2$)(Me$_2$bpy)] show enhancement of bands due to both ligand, suggesting that because the ligand LUMOs are very close in energy, a population of the molecules with MLCT to bpy/phen and a population of molecules with MLCT to bpy(Mes)$_2$ exist simultaneously.

■ ASSOCIATED CONTENT

⑤ Supporting Information

X-ray crystallographic data for the Cu(I) complexes in CIF format. Crystal structure refinement data, resonance Raman spectra, Cartesian coordinates of all the optimized geometries, and calculated frontier molecular orbitals of the complexes. This material is available free of charge via the Internet at http://pubs.acs.org.

■ AUTHOR INFORMATION

Corresponding Author
*E-mail: kgordon@chemistry.otago.ac.nz.

Notes

The authors declare no competing financial interest.

■ ACKNOWLEDGMENTS

■ REFERENCES

(1) Lavie-Cambot, A.; Cantuel, M.; Leydet, Y.; Jonusauskas, G.; Bassani, D. M.; McClenaghan, N. D. *Coord. Chem. Rev.* **2008**, *252*, 2572−2584.

(2) Scaltrito, D. V.; Thompson, D. W.; O'Callaghan, J. A.; Meyer, G. J. *Coord. Chem. Rev.* **2000**, *208*, 243−266.

(3) Robertson, N. *ChemSusChem* **2008**, *1*, 977−979.

(4) Armaroli, N. *Chem. Soc. Rev.* **2001**, *30*, 113−124.

(5) Lu, X.; Wei, S.; Wu, C.-M. L.; Li, S.; Guo, W. *J. Phys. Chem. C* **2011**, *115*, 3753−3761.

(6) Bessho, T.; Constable, E. C.; Graetzel, M.; Hernandez Redondo, A.; Housecroft, C. E.; Kylberg, W.; Nazeeruddin, M. K.; Neuburger, M.; Schaffner, S. *Chem. Commun.* **2008**, 3717−3719.

(7) Breddels, P. A.; Blasse, G.; McMillin, D. R. *Ber. Bunsenges. Phys. Chem.* **1984**, *88*, 572−578.

(8) Graetzel, M. *Acc. Chem. Res.* **2009**, *42*, 1788−1798.

(9) Hagfeldt, A.; Boschloo, G.; Sun, L.; Kloo, L.; Pettersson, H. *Chem. Rev.* **2010**, *110*, 6595−6663.

(10) Constable, E. C.; Redondo, A. H.; Housecroft, C. E.; Neuburger, M.; Schaffner, S. *Dalton Trans.* **2009**, 6634−6644.

(11) Bozic-Weber, B.; Constable, E. C.; Housecroft, C. E.; Neuburger, M.; Price, J. R. *Dalton Trans.* **2010**, *39*, 3585−3594.

(12) Bozic-Weber, B.; Constable, E. C.; Housecroft, C. E.; Kopecky, P.; Neuburger, M.; Zampese, J. A. *Dalton Trans.* **2011**, *40*, 12584−12594.

(13) Lei, Y.; Anson, F. C. *Inorg. Chem.* **1995**, *34*, 1083−1089.

(14) Schmittel, M.; Ganz, A. *Chem. Commun.* **1997**, 999−1000.

(15) Schmittel, M.; Luning, U.; Meder, M.; Ganz, A.; Michel, C.; Herderich, M. *Heterocycl. Commun.* **1997**, *3*, 493−498.

(16) Schmittel, M.; Ganz, A.; Fenske, D.; Herderich, M. *J. Chem. Soc., Dalton Trans.* **2000**, 353−359.

(17) Schmittel, M.; Michel, C.; Liu, S.-X.; Schildbach, D.; Fenske, D. *Eur. J. Inorg. Chem.* **2001**, *2001*, 1155−1166.

(18) Schmittel, M.; Kalsani, V.; Fenske, D.; Wiegrefe, A. *Chem. Commun.* **2004**, 490−491.

(19) Schmittel, M.; Kalsani, V.; Kishore, R. S. K.; Collfen, H.; Bats, J. W. *J. Am. Chem. Soc.* **2005**, *127*, 11544−11545.

(20) Schmittel, M.; Mahata, K. *Chem. Commun.* **2008**, 2550−2552.

(21) Schmittel, M.; He, B.; Fan, J.; Bats, J. W.; Engeser, M.; Schlosser, M.; Deiseroth, H. J. *Inorg. Chem.* **2009**, *48*, 8192−8200.

(22) Schmittel, M.; Mahata, K. *Inorg. Chem.* **2009**, *48*, 822−824.

(23) Mahata, K.; Saha, M. L.; Schmittel, M. *J. Am. Chem. Soc.* **2010**, *132*, 15933−15935.

(24) Fan, J.; Lal Saha, M.; Song, B.; Schonherr, H.; Schmittel, M. *J. Am. Chem. Soc.* **2012**, *134*, 150−153.

(25) Lazorski, M. S.; Gest, R. H.; Elliott, C. M. *J. Am. Chem. Soc.* **2012**, *134*, 17466−17469.

(26) Pellegrin, Y.; Sandroni, M.; Blart, E.; Planchat, A.; Evain, M.; Bera, N. C.; Kayanuma, M.; Sliwa, M.; Rebarz, M.; Poizat, O.; Daniel, C.; Odobel, F. *Inorg. Chem.* **2011**, *50*, 11309−11322.

(27) McMillin, D. R.; Kirchhoff, J. R.; Goodwin, K. V. *Coord. Chem. Rev.* **1985**, *64*, 83−92.

(28) Palmer, C. E. A.; McMillin, D. R.; Kirmaier, C.; Holten, D. *Inorg. Chem.* **1987**, *26*, 3167−3170.

(29) Crane, D. R.; DiBenedetto, J.; Palmer, C. E. A.; McMillin, D. R.; Ford, P. C. *Inorg. Chem.* **1988**, *27*, 3698−3700.

(30) Stacy, E. M.; McMillin, D. R. *Inorg. Chem.* **1990**, *29*, 393−396.

(31) Everly, R. M.; McMillin, D. R. *Photochem. Photobiol.* **1989**, *50*, 711−716.

(32) Chen, L. X.; Shaw, G. B.; Novozhilova, I.; Liu, T.; Jennings, G.; Attenkofer, K.; Meyer, G. J.; Coppens, P. *J. Am. Chem. Soc.* **2003**, *125*, 7022−7034.

(33) Siddique, Z. A.; Yamamoto, Y.; Ohno, T.; Nozaki, K. *Inorg. Chem.* **2003**, *42*, 6366−6378.

(34) Vorontsov, I. I.; Graber, T.; Kovalevsky, A. Y.; Novozhilova, I. V.; Gembicky, M.; Chen, Y.-S.; Coppens, P. *J. Am. Chem. Soc.* **2009**, *131*, 6566−6573.

(35) Shaw, G. B.; Grant, C. D.; Shirota, H.; Castner, E. W.; Meyer, G. J.; Chen, L. X. *J. Am. Chem. Soc.* **2007**, *129*, 2147−2160.

(36) Iwamura, M.; Takeuchi, S.; Tahara, T. *J. Am. Chem. Soc.* **2007**, *129*, 5248−5256.

(37) Iwamura, M.; Watanabe, H.; Ishii, K.; Takeuchi, S.; Tahara, T. *J. Am. Chem. Soc.* **2011**, *133*, 7728−7736.

(38) Fraser, M. G.; van der Salm, H.; Cameron, S. A.; Barnsley, J. E.; Gordon, K. C. *Polyhedron* **2012**, DOI: 10.1016/j.poly.2012.08.001.

(39) Schmittel, M.; Ganz, A.; Schenk, W. A.; Hagel, M. *Z. Naturforsch. B* **1999**, *54b*, 559−564.

(40) Israel, R. J.; Murray, R. K. *J. Org. Chem.* **1985**, *50*, 1573−1577.

(41) Howell, S. L.; Scott, S. M.; Flood, A. H.; Gordon, K. C. *J. Phys. Chem. A* **2005**, *109*, 3745−3753.

(42) Shriver, D. F.; Dunn, J. B. R. *Appl. Spectrosc.* **1974**, *28*, 319−23.

(43) Lind, S. J.; Gordon, K. C.; Waterland, M. R. *J. Raman Spectrosc.* **2008**, *39*, 1556−1567.

(44) Cleland, D. M.; Irwin, G.; Wagner, P.; Officer, D. L.; Gordon, K. C. *Chem.—Eur. J.* **2009**, *15*, 3682−3690.

(45) Lind, S. J.; Walsh, T. J.; Blackman, A. G.; Polson, M. I. J.; Irwin, G. I. S.; Gordon, K. C. *J. Phys. Chem. A* **2009**, *113*, 3566−3575.

(46) Fraser, M. G.; Blackman, A. G.; Irwin, G. I. S.; Easton, C. P.; Gordon, K. C. *Inorg. Chem.* **2010**, *49*, 5180−5189.

(47) Fraser, M. G.; Clark, C. A.; Horvath, R.; Lind, S. J.; Blackman, A. G.; Sun, X.-Z.; George, M. W.; Gordon, K. C. *Inorg. Chem.* **2011**, *50*, 6093−6106.

(48) Frost, K. J.; McCreery, R. L. *Appl. Spectrosc.* **1998**, *52*, 1614−1618.

(49) McCreery, R. L. *Raman Spectroscopy for Chemical Analysis*; John Wiley & Sons, Inc.: New York, 2000.

(50) Lee, C.; Yang, W.; Parr, R. G. *Phys. Rev. B* **1988**, *37*, 785−789.

(51) Becke, A. D. *J. Chem. Phys.* **1993**, *98*, 1372−1377.

(52) Petersson, G. A.; Tensfeldt, T. G.; J. A. Montgomery, J. *J. Chem. Phys.* **1991**, *94*, 6091−6101.

(53) Hay, P. J.; Wadt, W. R. *J. Chem. Phys.* **1985**, *82*, 299−310.

(54) Walsh, P. J.; Gordon, K. C.; Lundin, N. J.; Blackman, A. G. *J. Phys. Chem. A* **2005**, *109*, 5933−5942.

(55) Howell, S. L.; Gordon, K. C.; Waterland, M. R.; Leung, K. H.; Phillips, D. L. *J. Phys. Chem. A* **2006**, *110*, 11194−11199.

(56) Frisch, M. J.; Trucks, G. W.; Schlegel, H. B.; Scuseria, G. E.; Robb, M. A.; Cheeseman, J. R.; Scalmani, G.; Barone, V.; Mennucci, B.; Petersson, G. A.; Nakatsuji, H.; Caricato, M.; Li, X.; Hratchian, H. P.; Izmaylov, A. F.; Bloino, J.; Zheng, G.; Sonnenberg, J. L.; M. Hada, M. E.; Toyota, K.; Fukuda, R.; Hasegawa, J.; Ishida, M.; Nakajima, T.; Honda, Y.; Kitao, O.; Nakai, H.; Vreven, T.; J. A. Montgomery, J.; Peralta, J. E.; Ogliaro, F.; Bearpark, M.; Heyd, J. J.; Brothers, E.; Kudin, K. N.; Staroverov, V. N.; Kobayashi, R.; Normand, J.; Raghavachari, K.; Rendell, A.; Burant, J. C.; Iyengar, S. S.; Tomasi, J.; Cossi, M.; Rega, N.; Millam, J. M.; Klene, M.; Knox, J. E.; Cross, J. B.; Bakken, V.; Adamo, C.; Jaramillo, J.; Gomperts, R.; Stratmann, R. E.; Yazyev, O.; Austin, A. J.; Cammi, R.; Pomelli, C.; Ochterski, J. W.; Martin, R. L.; Morokuma, K.; Zakrzewski, V. G.; Voth, G. A.; Salvador, P.; Dannenberg, J. J.; Dapprich, S.; Daniels, A. D.; Farkas, Ö.; Foresman, J. B.; Ortiz, J. V.; Cioslowski, J.; Fox, D. J. *Gaussian 09*; Gaussian, Inc.: Wallingford CT, 2009.

(57) Earles, J. C.; Gordon, K. C.; Officer, D. L.; Wagner, P. *J. Phys. Chem. A* **2007**, *111*, 7171−7180.

(58) Horvath, R.; Gordon, K. C. *Coord. Chem. Rev.* **2010**, *254*, 2505−2518.

(59) Horvath, R.; Gordon, K. C. *Inorg. Chim. Acta* **2011**, *374*, 10−18.

(60) Guirgis, G. A.; Nashed, Y. E.; Durig, J. R. *J. Mol. Struct.* **1999**, *510*, 13−34.

(61) Guirgis, G. A.; Nashed, Y. E.; Durig, J. R. *Spectrochim. Acta Part A* **2000**, *56*, 1065−1078.

(62) Durig, J. R.; Xiao, J.; Robb, J. B., II; Daeyaert, F. F. D. *J. Raman Spectrosc.* **1998**, *29*, 463−472.

(63) Yang, L.; Powell, D. R.; Houser, R. P. *Dalton Trans.* **2007**, 955−964.

(64) Burnett, M. N.; Johnson, C. K. *Oak Ridge National Laboratory Report ORNL-6895*; Oak Ridge National Laboratory: Oak Ridge, TN, 1996.

(65) Janiak, C. *J. Chem. Soc., Dalton Trans.* **2000**, 3885−3896.

(66) Klemens, F. K.; Palmer, C. E. A.; Rolland, S. M.; Fanwick, P. E.; McMillin, D. R.; Sauvage, J. P. *New J. Chem.* **1990**, *14*, 129.

(67) Eggleston, M. l. K.; Fanwick, P. E.; Pallenberg, A. J.; McMillin, D. R. *Inorg. Chem.* **1997**, *36*, 4007−4010.

(68) Burke, P. J.; Henrick, K.; McMillin, D. R. *Inorg. Chem.* **1982**, *21*, 1881−1886.

(69) Dobson, J.; Green, B.; Healy, P.; Kennard, C.; Pakawatchai, C.; White, A. *Aust. J. Chem.* **1984**, *37*, 649−659.

(70) Healy, P. C.; Engelhardt, L. M.; Patrick, V. A.; White, A. H. *J. Chem. Soc., Dalton Trans.* **1985**, *0*, 2541−2545.

(71) Miller, M. T.; Gantzel, P. K.; Karpishin, T. B. *Inorg. Chem.* **1998**, *37*, 2285−2290.

(72) Miller, M. T.; Gantzel, P. K.; Karpishin, T. B. *Angew. Chem., Int. Ed.* **1998**, *37*, 1556−1558.

(73) Miller, M. T.; Gantzel, P. K.; Karpishin, T. B. *Inorg. Chem.* **1999**, *38*, 3414−3422.

(74) Miller, M. T.; Gantzel, P. K.; Karpishin, T. B. *J. Am. Chem. Soc.* **1999**, *121*, 4292−4293.

(75) Ali, B. F.; Al-sou'od, K.; Al-Ja'ar, N.; Nassar, A.; Zaghal, M. H.; Judeh, Z.; Al-Far, R.; Al-Refai, M.; Ibrahim, M.; Mansi, K.; Al-Obaidi, K. H. *J. Coord. Chem.* **2006**, *59*, 229−241.

(76) Al-Obaidi, A. H. R.; Gordon, K. C.; McGarvey, J. J.; Bell, S. E. J.; Grimshaw, J. *J. Phys. Chem.* **1993**, *97*, 10942−10947.

(77) Jahng, Y.; Hazelrigg, J.; Kimball, D.; Riesgo, E.; Wu, F.; Thummel, R. P. *Inorg. Chem.* **1997**, *36*, 5390−5395.

(78) Dreuw, A.; Head-Gordon, M. *J. Am. Chem. Soc.* **2004**, *126*, 4007−4016.

(79) Bradley, P. G.; Kress, N.; Hornberger, B. A.; Dallinger, R. F.; Woodruff, W. H. *J. Am. Chem. Soc.* **1981**, *103*, 7441−7446.

(80) Henry, W.; Coates, C. G.; Brady, C.; Ronayne, K. L.; Matousek, P.; Towrie, M.; Botchway, S. W.; Parker, A. W.; Vos, J. G.; Browne, W. R.; McGarvey, J. J. *J. Phys. Chem. A* **2008**, *112*, 4537−4544.

(81) Sauvage, J. P.; Collin, J. P.; Chambron, J. C.; Guillerez, S.; Coudret, C.; Balzani, V.; Barigelletti, F.; De Cola, L.; Flamigni, L. *Chem. Rev.* **1994**, *94*, 993−1019.

(82) McCusker, J. K. *Acc. Chem. Res.* **2003**, *36*, 876−887.

(83) Gordon, K. C.; McGarvey, J. J. *Inorg. Chem.* **1991**, *30*, 2986−2989.

(84) Gordon, K. C.; McGarvey, J. J. *Chem. Phys. Lett.* **1989**, *162*, 117−122.

(85) McGarvey, J. J.; Bell, S. E. J.; Gordon, K. C. *Inorg. Chem.* **1988**, *27*, 4003−4006.

(86) Reish, M. E.; Kay, A. J.; Teshome, A.; Asselberghs, I.; Clays, K.; Gordon, K. C. *J. Phys. Chem. A* **2012**, *116*, 5453−5463.

(87) Elliott, A. B. S.; Horvath, R.; Gordon, K. C. *Chem. Soc. Rev.* **2012**, *41*, 1929−1946.

(88) Horvath, R.; Otter, C. A.; Gordon, K. C.; Brodie, A. M.; Ainscough, E. W. *Inorg. Chem.* **2010**, *49*, 4073−4083.

(89) Gordon, K. C.; Burrell, A. K.; Simpson, T. J.; Page, S. E.; Kelso, G.; Polson, M. I. J.; Flood, A. *Eur. J. Inorg. Chem.* **2002**, *2002*, 554−563.

(90) Clark, R. J. H.; Dines, T. J. *Angew. Chem.* **1986**, *98*, 131−160.

(91) Hirakawa, A. Y.; Tsuboi, M. *Science* **1975**, *188*, 359−361.

(92) Parker, W. L.; Crosby, G. A. *J. Phys. Chem.* **1989**, *93*, 5692−5696.

(93) Williams, R. M.; Cola, L. D.; Hartl, F.; Lagref, J.-J.; Planeix, J.-M.; Cian, A. D.; Hosseini, M. W. *Coord. Chem. Rev.* **2002**, *230*, 253−261.

(94) Briggs, B. N.; Durola, F.; McMillin, D. R.; Sauvage, J.-P. *Can. J. Chem.* **2011**, *89*, 98−103.

(95) Riesgo, E. C.; Hu, Y.-Z.; Bouvier, F. d. r.; Thummel, R. P.; Scaltrito, D. V.; Meyer, G. J. *Inorg. Chem.* **2001**, *40*, 3413−3422.